Journal of
Composites Science

MDPI

Article

Damping Properties of Hybrid Composites Made from Carbon, Vectran, Aramid and Cellulose Fibers

Hauke Kröger, Stephan Mock, Christoph Greb * and Thomas Gries

Institut für Textiltechnik, RWTH Aachen University, 52074 Aachen, Germany;
hauke.kroeger@ita.rwth-aachen.de (H.K.); stephan.mock@rwth-aachen.de (S.M.);
Thomas.Gries@ita.rwth-aachen.de (T.G.)
* Correspondence: christoph.greb@ita.rwth-aachen.de

Abstract: Hybridization of carbon fiber composites can increase the material damping of composite parts. However, there is little research on a direct comparison of different fiber materials—particularly for carbon fiber intraply-hybrid composites. Hence, the mechanical- and damping properties of different carbon fiber intraply hybrids are analyzed in this paper. Quasi unidirectional fabrics made of carbon, aramid, Vectran and cellulose fibers are produced, and their mechanical properties are analyzed. The material tests show an increased material damping due to the use of Vectran and aramid fibers, with a simultaneous reduction in strength and stiffness.

Keywords: composite; hybrid composite; damping; intraply hybrid; carbon fiber

check for updates

Citation: Kröger, H.; Mock, S.; Greb, C.; Gries, T. Damping Properties of Hybrid Composites Made from Carbon, Vectran, Aramid and Cellulose Fibers. *J. Compos. Sci.* **2022**, *6*, 13. https://doi.org/10.3390/jcs6010013

Academic Editor: Jiadeng Zhu

Received: 2 December 2021
Accepted: 24 December 2021
Published: 31 December 2021

1. Introduction

Vibrations have a harmful effect on the human body. In the field of occupational safety, attention has been drawn to the topic for a long time. However, harmful vibrations also occur in recreational activities when using sports equipment. This also includes bicycles, the use of which can lead to potentially harmful vibrations for the user [1]. Carbon fiber reinforced composites are a popular material for the construction of bicycles due to their excellent lightweight properties. Vibrations are transmitted to the cyclists via composite components but can be reduced by increasing the material damping of the composites. Material damping causes a conversion of vibrational energy into (mostly) thermal energy by internal friction [2].

The material damping of composites is determined by the damping of the matrix and the fibers, as well as their arrangement, connection and interphase [3]. The matrix has a greater influence on the damping of the composite than the fibers [4]. Nonetheless, many applications do not allow for a change in matrix material or change of the interphase between fibers and matrix. An increase in damping can therefore only be achieved by the fibers. This requires a change in fiber type [3], fiber orientation, respectively, laminate construction [5–7] or fiber volume content [8].

In particular, the use of fiber types with high inherent self-damping offers great potential for increasing the material damping of carbon fiber composites. Yet, the fibers in question have too little stiffness or strength to produce a lightweight composite consisting entirely out of high damping fibers. This problem can be addressed by hybridization: ordinary reinforcing fibers (e.g., carbon fibers) are combined with fibers with high self-damping within a composite.

A hybrid composite consists of two or more different types of fibers. A distinction is made between hybridization on the laminate level (*interply*), on the roving level (*intraply*) or on the filament level (*intrayarn*), the schematic structure is shown in Figure 1 [9]. In addition, mixed forms of the above-mentioned hybridization types are possible. The aim of hybridization is to improve certain properties (e.g., increased damping) disproportionately to the loss of other properties (e.g., decreased stiffness) [10], which is referred to as positive synergy effects.

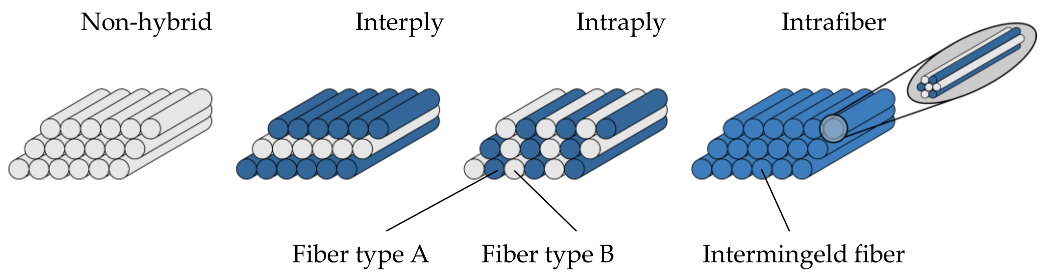

Figure 1. Hybridization types of composites in comparison.

A main characteristic of hybridization is the dispersion of the different fiber types; the higher the dispersion, the higher the synergy effects achieved [11]. The dispersion depends largely on the type of hybridization used, but can also be influenced by the fiber diameter or the ply thickness [12,13]. For a given lay-up and fiber diameter, the best dispersion is achieved by an intrafiber hybrid. Interply hybridization offers the lowest dispersion, while intraply is a good trade-off between Intrayarn and interply hybrids [10,14].

The main focus of research in the field of hybrid composites has been on the following areas: Increasing the elongation at break or creating a pseudo ductile fracture behavior [12,15,16], improving static strength [17] and fatigue strength [18–20], cost reduction through the integration of low-cost fiber types [21] and improvements in impact properties [14,22–24]. There is comparatively less research activity in the area of damping enhancement through hybridization [25]. In this context, the most research results were reported on investigations of the damping properties of natural fiber hybrid composites:

Ashtworth et al. demonstrated an increase in damping by using jute fibers in an interply hybrid with carbon fibers [26]. Assarar et al. and Guen et al. achieved an increase in damping using a flax-carbon interply hybrid [27,28]. Other authors showed an increase in damping by hybridizing glass fiber laminates with flax fibers [29,30] or kenaf fibers [31]. Although natural fibers allow an increase in material damping, they also have central deficits that make their use in high-performance composites—such as bicycles—unattractive. In particular, the inconsistent fiber properties and the absorption of the resin are major deficits [32]. Synthetic fibers with good damping properties could overcome the disadvantages of natural fibers. However, there is very little research activity on increasing the damping of hybrid (carbon fiber) composites using synthetic fibers. Especially the increase of material damping by intraply hybridization has been investigated very little. The increase of material damping by using certain synthetic fibers have been shown by different authors, although not within the context of hybrid composites: Studies showed an increase in damping by using aramid fibers [33] and cellulose fibers [34]. Liquid crystalline polymer (LCP) materials are also known for their good damping properties [35]. Therefor the scope of this work is to investigate the manufacturability and mechanical properties of intraply hybrid composites made of carbon and synthetic fibers. The aim is to use the novel hybrid composites as a material for the manufacture of bicycle components in order to reduce the vibration load on the human body.

2. Materials and Methods

2.1. Materials

Three different unidirectional hybrids and a non-hybrid reference made from carbon fibers were investigated. The investigations commenced with the production of quasi unidirectional fabrics, which were further processed into composites using the vacuum infusion process. An intraply level hybridization was chosen, as this allows a good compromise between dispersion and efficient and economical production. The fabrics were produced on a weaving machine. As shown in Figure 2 all reinforcing fibers were oriented in warp direction and connected in weft direction by a 10 tex polyester fiber.

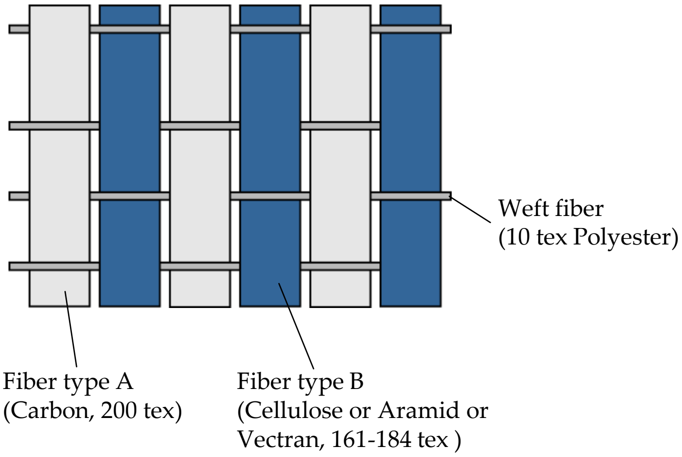

Figure 2. Construction of unidirectional hybrid textiles.

The weft thread only serves as a fixation of the warp threads and leads to very low ondulations, which are not comparable to the ondulations of a classical woven fabric. Therefore, the final product is a fabric with a unidirectional (UD) arrangement of the reinforcing fibers. The hybrid fabrics produced each consist of two types of fibers: on the one hand, carbon fibers to generate strength and stiffness and, on the other hand, functional fibers to generate the damping effect. The functional fibers investigated are aramid, cellulose and fibers made of liquid crystalline polymer (LCP) (Vectran®). The properties of the fibers are shown in Table 1.

Table 1. Properties of the fibers used.

Material	**Manufacturer and Product Name**	**Density [g/cm³]**	**Tensile Modulus [GPa]**	**Tensile Strength [MPa]**
Carbon	Teijin HTS 45	1.76	245	4500
Aramid	Teijin Twaron® 2200	1.45	100	2240
LCP/Vectran	Kuraray Vectran® HTME	1.4	75	3200
Cellulose	Cordenka 700	1.5	14.4	778

The design of the UD-fabric was based on HTS 45 type carbon fibers with a fineness of 200 tex. The fineness of the functional fibers was selected in such a way that (ideally) a ratio of 50 volume% carbon fiber to 50 volume% functional fibers is achieved in the hybrid UD fabric. This ensures the best possible dispersion under the given boundary conditions (fineness of the carbon fibers). The properties of the UD fabrics are shown in Table 2.

The different fiber types were arranged in warp direction according to the following pattern: $A, B, A, B, A, \ldots$. A plain weave was used, with one weft thread per centimeter of warp length. The low weft density resulted in an ondulation of the fabric in the weft direction. This does not influence the properties in fiber direction, respectively, warp direction—in warp direction the fibers are parallel and unidirectional. Figure 3 shows the UD-fabrics produced.

Table 2. Properties of the dry UD-fabrics.

Textile Name	Fiber A	Fiber B	Volume Content Fiber A [%]	Volume Content Fiber B [%]	Arial Weight [g/m^2]
CaCa	Carbon	Carbon	50	50	200
CaAr	Carbon	Aramid	50.4	49.6	180
CaVe	Carbon	Vectran	48.8	51.2	185
CaCe	Carbon	Cellulose	48.1	51.9	192

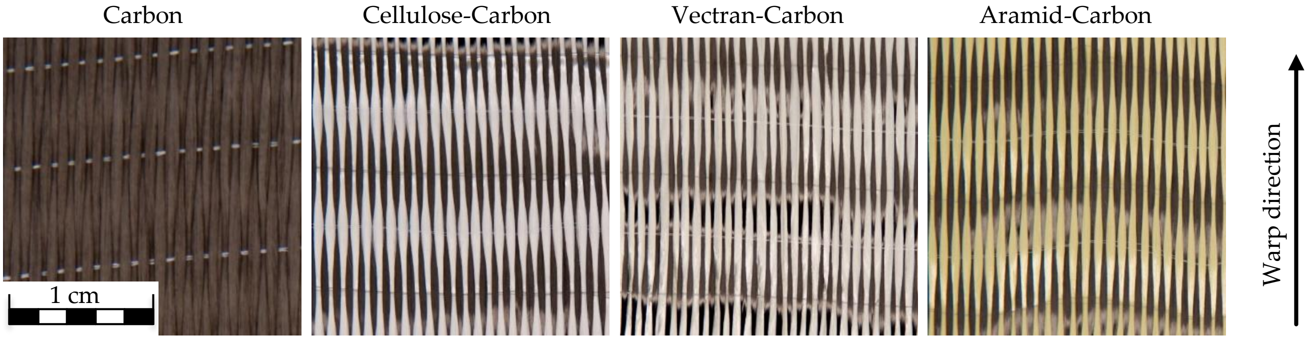

Figure 3. Hybrid and non-hybrid UD-fabrics produced.

The UD fabrics were then used to make composite panels using a vacuum infusion process. An epoxy thermoset resin of the type of Hexion RIM R426/RIM H35 was used. For the tensile and damping tests, plates were made from five layers of each hybrid fabric type, while the bending test specimens were made from nine layers of each UD fabric type. All layers were arranged in the 0° direction. After the infusion, the plates were tempered at 80 °C for two hours, followed by the final cutting of the test specimens. Table 3 shows the properties of the composite specimens for tensile and damping testing. The density was calculated from the specimen size and weight. The fiber volume content was calculated from the layup, the size of the composite plates and the densities of the individual components.

Table 3. Properties of specimens for tensile and damping testing.

Composite Name	Layup	Density [g/cm^3]	Thickness [mm]	Fiber Volume Content [Vol%]
Carbon	$5 \times [\mathrm{CaCa}_{0^\circ}]$	1.41	1.28	47
Aramid-Carbon	$5 \times [\mathrm{CaAr}_{0^\circ}]$	1.33	1.36	49
Vectran-Carbon	$5 \times [\mathrm{CaVe}_{0^\circ}]$	1.24	1.38	46
Cellulose-Carbon	$5 \times [\mathrm{CaCe}_{0^\circ}]$	1.35	1.35	46

For quality control of the manufacturing process, interlaminar shear strength (ILSS) tests were carried out, which showed a low interlaminar strength of samples made of Vectran-Carbon UD-fabrics. The Vectran-Carbon fabrics were therefor plasma treated, to improve the surface properties of the Vectran fibers regarding the adhesion of the epoxy matrix.

2.2. Methods

The material properties of the composites were determined by tensile-, flexural- and damping tests. The tensile tests were carried out in accordance with DIN EN ISO 527-5, with tabs were attached to the specimens. The elongation was measured using a video extensometer. Only plasma-treated Vectran-Carbon hybrids were used in the tensile tests. Test specimens for tensile tests were 250 mm long, 20 mm wide and approximately one millimeter thick.

The flexural tests were carried out in accordance with DIN EN ISO 14125. The dimensions were length = 100 mm, width = 15 mm, and thickness = 2.1 mm to 2.6 mm (depending on the fabric type). The distance between the supports was 91 mm. ILSS tests were carried out according to DIN EN ISO 14130, but were only used for quality control, hence the results are not discussed in further detail.

The material damping was measured via the logarithmic decrement (Λ), which is determined from the step response of a cantilever beam in free-fixed configuration. The logarithmic decrement is defined as the ratio of the amplitudes (y) of two adjacent amplitudes of a damped oscillation (see Equation (1)).

$$\Lambda = \ln \frac{y_i}{y_{i+1}} \quad (1)$$

The determination was carried out on an apparatus as shown in Figure 4 that is based on the development of Romano [36]. The specimens are firmly clamped at one end, while the opposite side is freely movable. The specimens are excited to vibrate by a single deflection and then oscillate at the natural frequency of the vibration system. The deflection is caused by a cam, which is operated by a hand lever and always deflects the specimen by the same distance. The (decaying) vibration amplitude and period duration are then recorded using a laser distance sensor and evaluated in MATLAB®.

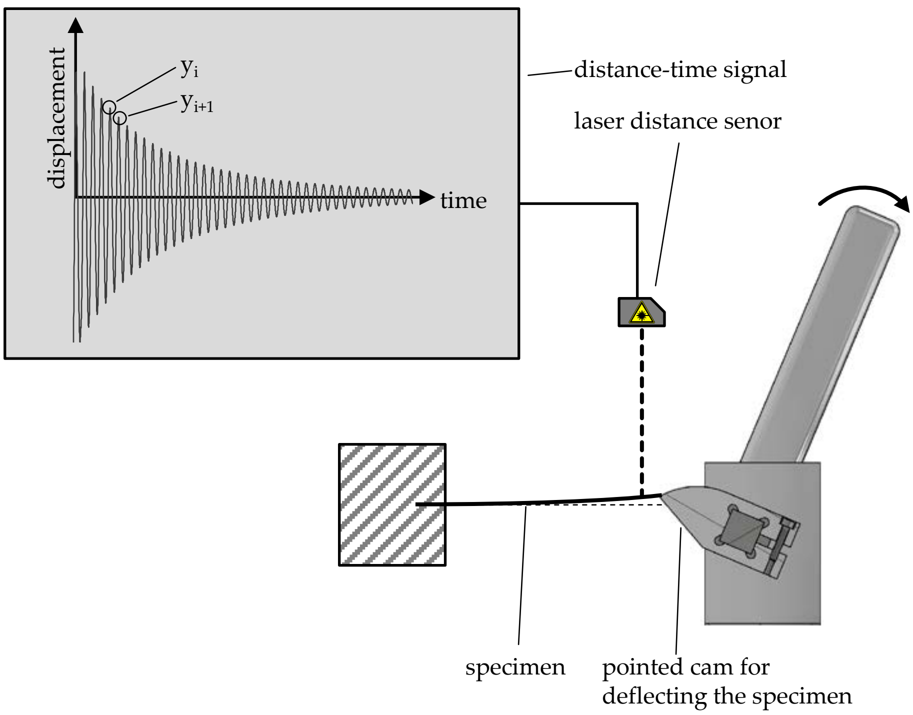

Figure 4. Apparatus for measuring material damping.

The damping was determined in the direction of the fibers. Since the vibration response (and thus also the determined damping) depends to a large extent on the stiffness of the beams, all samples were tested with the same spring stiffness. By changing the free length, the spring stiffness of the specimen is changed. The spring stiffness is based on the material stiffness, the free length and the test specimen cross-section. It can be easily determined by

Equation (2), with the spring stiffness (c), the acting force (F) and the resulting maximum deflection (s).

$$c = F/s \tag{2}$$

To adjust the spring stiffness, the free ends of the test specimens were weighted with a (constant) weight and the free length was changed until a deflection of 10.4 mm was achieved.

3. Results and Discussion

All results presented below are found to be significantly different (alpha = 5%). All error bars describe the extent of one standard deviation of the respective test. Seven test specimens were tested per test series.

3.1. Strength

The following Figure 5 shows the tensile strength and flexural strength of the composite specimens in fiber direction. In the following assessment, the specimens are referred to by the types of fibers used, e.g., *Carbon* refers to composite specimens made from a plain carbon fabric, *Vectran-Carbon* refers to specimens made from a hybrid vectran-carbon fabric.

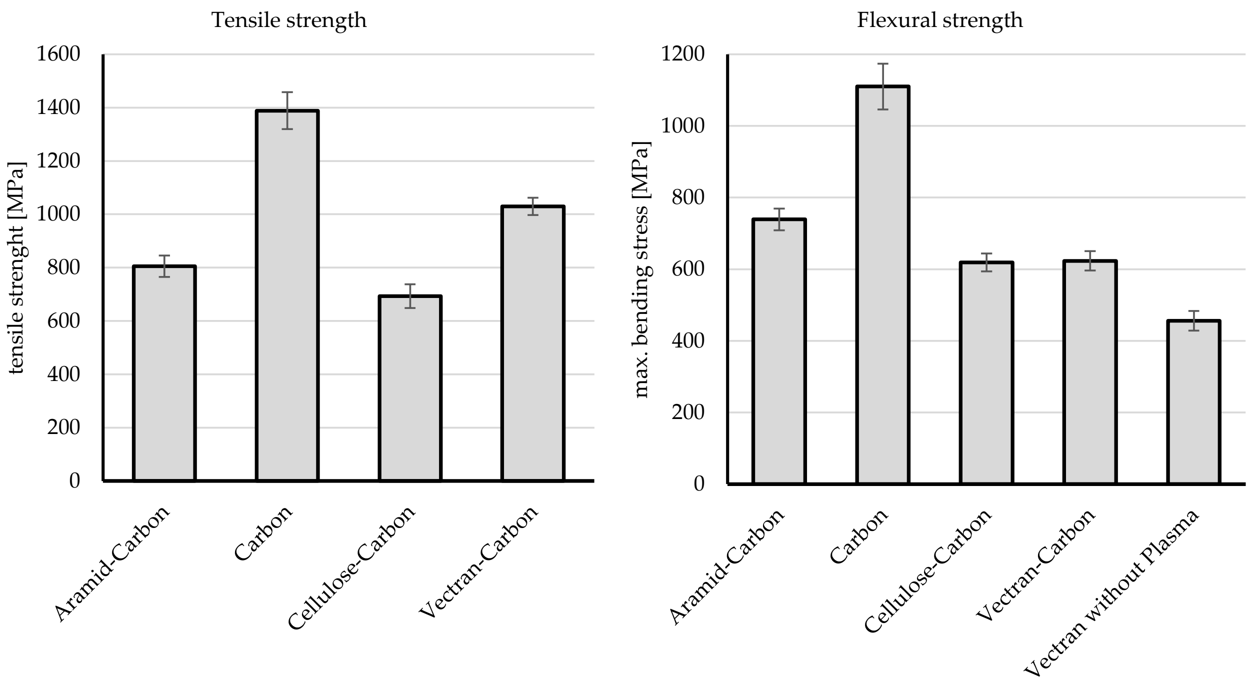

Figure 5. Strength in tensile and flexural direction.

Carbon shows the highest tensile- and flexural strength, Cellulose-Carbon the lowest. The tensile strengths of the composite specimens correlates with the tensile strengths of the individual fibers (see Table 1). The results for the tensile strength compared to the flexural strength show a different material behavior in relation to aramid- and (plasma treated) Vectran fibers.

Vectran-Carbon has the second highest tensile strength but only the third highest flexural strength, while Aramid-Carbon has the third highest tensile strength and the second highest flexural strength. These differences are particularly evident in Vectran-Carbon, which has a 25% lower tensile strength than Carbon but a 44% lower flexural strength. This material behavior could be an indication of a reduced compressive strength of the Vectran fibers or—despite plasma treatment—a low fiber-matrix adhesion of the Vectran fibers.

The fracture behavior in the comparison between tensile- and flexural-tests is consistent. Carbon and Cellulose-Carbon samples break brittle. Whereas Aramid-Carbon and Vectran-Carbon have a certain residual strength, as the majority of the aramid- or Vectran fibers are still intact after the failure of the specimen. Figure 6 shows the stress-displacement curve of representative specimens of each material during flexural tests.

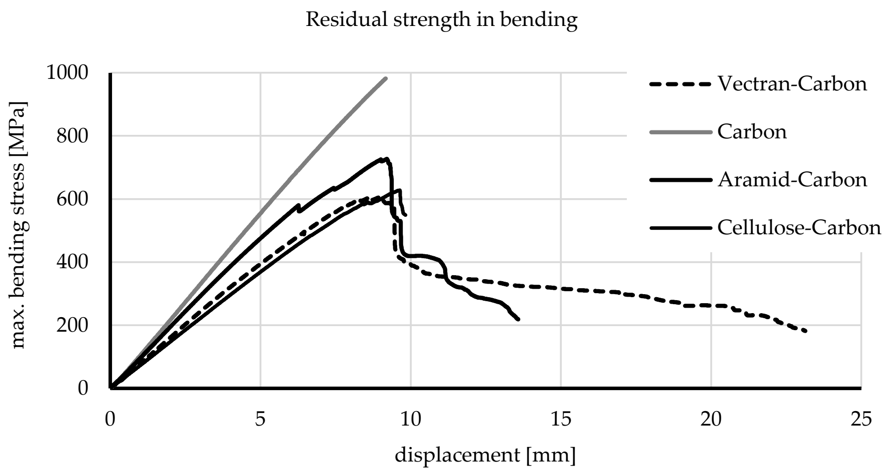

Figure 6. Fracture behavior under flexural loading.

The brittle failure of Carbon and Cellulose-Carbon is evident. After reaching the maximum stress, the whole specimen breaks suddenly and brittle. In the case of Vectran-Carbon and Aramid-Carbon, the carbon fibers break first when the maximum force is reached. The Vectran or aramid fibers, however, do not break yet due to their higher elongation at break and allow the composite to retain a certain residual strength.

3.2. Surface Treament of Vectran Fibers

Plasma treatment of Vectran fibers has produced a significant improvement in fiber-matrix adhesion. This is shown by the result of the bending strength of Vectran-Carbon vs. Vectran(-Carbon) without plasma; the use of plasma treatment improved the bending strength by 35%. A comparison of computer tomography (CT) scans supports this thesis. Figure 7 shows CT scans in the thickness direction of the bending test specimens made of (plasma) treated and untreated Vectran-Carbon in comparison to specimens from Carbon textiles.

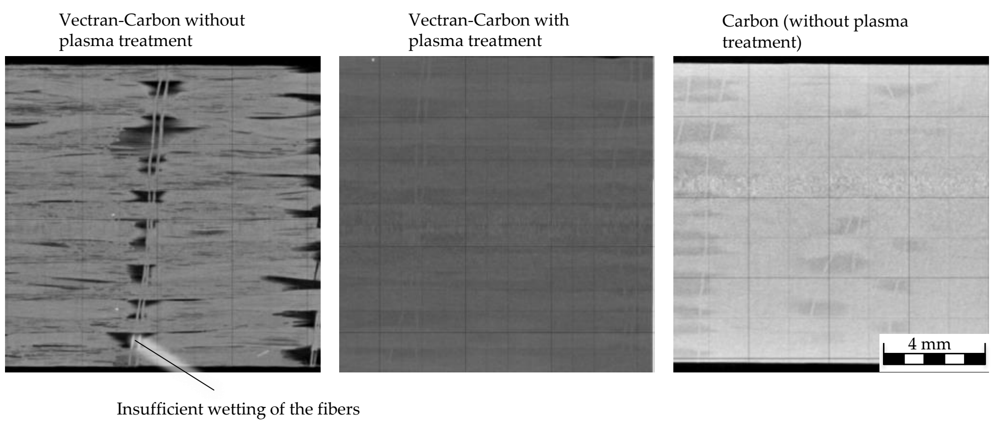

Figure 7. CT scans of Vectran-Carbon composite and Carbon composites.

Untreated Vectran-Carbon shows non-impregnated areas. Whereas plasma-treated Vectran-Carbon shows an impregnation comparable to that of Carbon.

3.3. Stiffness

The following Figure 8 shows the tensile moduli in fiber direction of the different hybrids and the Carbon reference.

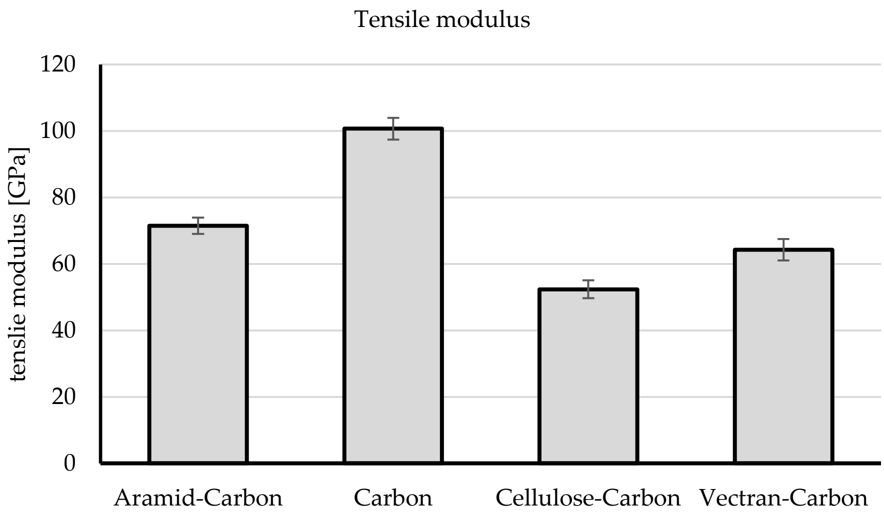

Figure 8. Tensile modulus in fiber direction.

A Carbon reinforcement leads to the highest stiffness, Cellulose-Carbon to the lowest. The tensile moduli of the composites also show a correlation with the moduli of the individual fibers.

3.4. Damping

The logarithmic decrement of the different samples—with the same spring stiffness—is shown below in Figure 9.

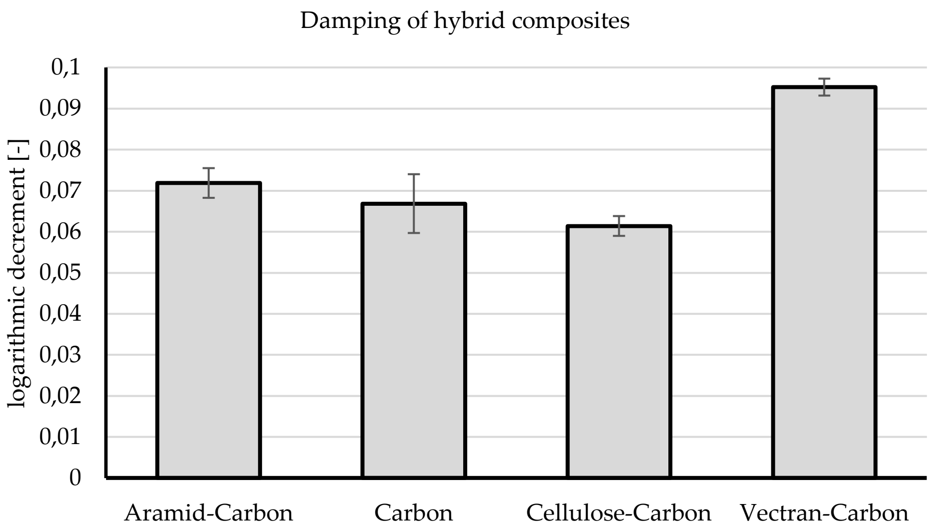

Figure 9. Logarithmic decrement with the same spring stiffness.

Specimens from Vectran-Carbon archive significantly higher damping than the Carbon reference. Aramid-Carbon and Cellulose-Carbon achieve similar values to Carbon. Whereby the damping of Aramid-Carbon is slightly higher than that of Carbon, while the damping of Cellulose-Carbon is slightly smaller than that of Carbon. To achieve the same spring stiffness (162 N/m), the tests were carried out at the free lengths as displayed in Table 4.

Table 4. Free length and damped natural frequency.

Material	Free Length [mm]	Frequency [Hz]
Aramid-Carbon	161	52
Carbon	164	53
Cellulose-Carbon	145	56
Vectran-Carbon	149	59

3.5. Density Specific Properties

The hybridization results in a reduction in the strength and stiffness of the composite, but at the same time also in a lower density of the overall composite compared to Carbon. Since the composites investigated are used for lightweight applications, the density must also be considered; the lower the density, the more of a material can be used. Through a density-specific consideration of the strength and stiffness, the decrease in strength and stiffness is less pronounced. Figure 10 shows the comparison between absolute and (density-) specific properties of the investigated materials. The area of the circles represents the amount of material damping. All data has been normalized to the respective properties of Carbon and is therefore given as a percentage.

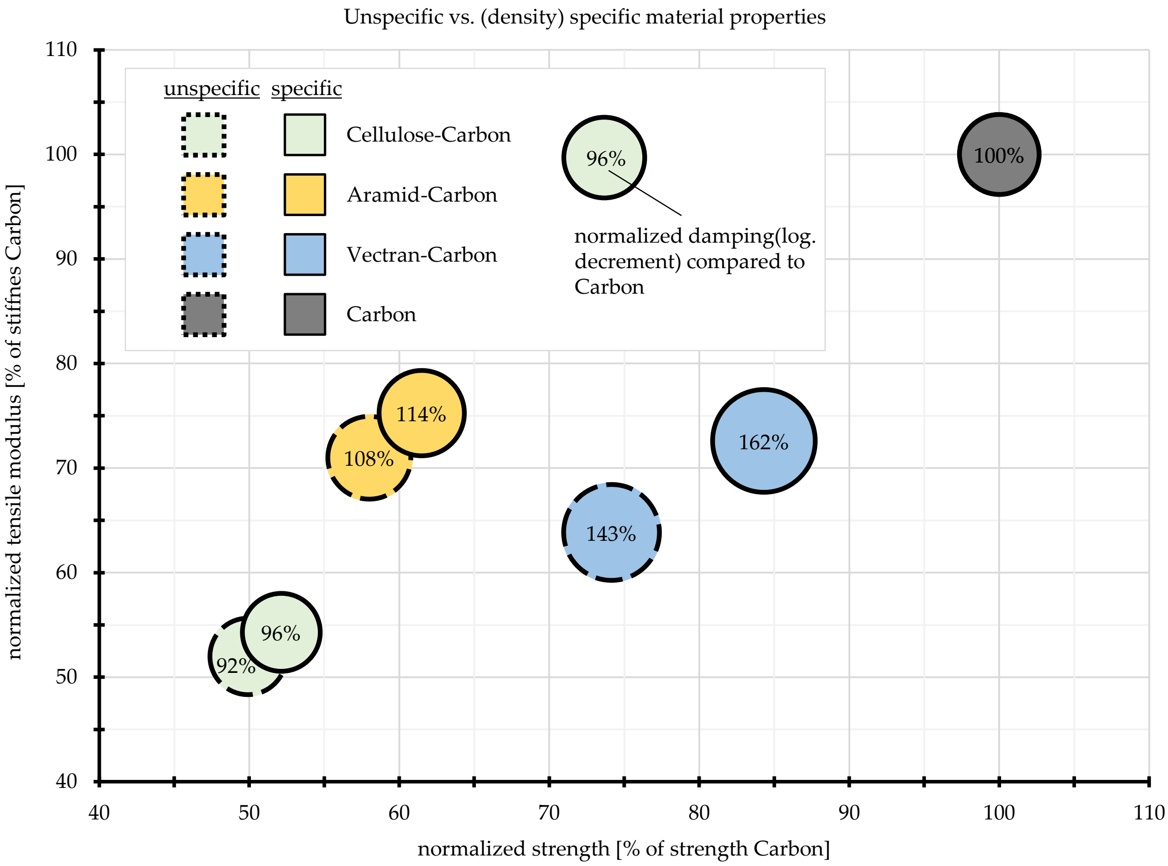

Figure 10. Effect of density on stiffness, strength and damping in fiber direction.

The specific consideration of strength, stiffness and damping reduces the difference between Carbon and the hybrid composites. The lower the density, the more pronounced the effect. By using hybrid composites, the damping can be increased over-proportionally to the *loss* of the mechanical properties.

3.6. Discussion of Mechanical Properties

The reason for the low strength of hybrid composites compared to carbon composites lies in the different stiffnesses and elongations at break of the individual fiber materials. The strength of the composites is dominated by carbon fibers, as these carry the higher load due to their high stiffness. Vectran-Carbon and Aramid-Carbon exhibit the same behavior: When subjected to a load, the carbon fibers and the aramid or Vectran fibers are elongated by the same amount. With increasing elongation, the tensile strength of the carbon fibers is exceeded first before the tensile strength of the Vectran or aramid fibers is reached. The reason for this is the lower stiffness and higher elongation at break of the Vectran or aramid fibers. The carbon fibers therefore fail first, with the result that the applied loads are now carried by the Vectran or aramid fibers. Due to the lower stiffness of the aramid and Vectran fibers, a drop in stress occurs in the specimens (see Figure 6). The specimens can be elongated even further until total failure. Overall, the Vectran-Carbon and Aramid-Carbon specimens achieve a higher elongation at break than the carbon specimens. However, the absolute tensile strength of the hybrid composite is lower than that of the pure carbon specimens since the hybrid specimens contain fewer—load bearing—carbon fibers overall.

The same behavior should theoretically apply to the Cellulose-Carbon specimens as the cellulose fibers have a very low stiffness as well as a very elongation at break. At the strain that leads to failure of the carbon fibers, stress in the cellulose fibers is still very much below their tensile strength. After the failure of the carbon fibers, there should be a stress drop in the specimen and the specimen should subsequently still have residual strength until failure. However, this is not the case, as the Cellulose-Carbon specimens fail brittly. The reason for this could be the interaction between the control of the testing machine and the strength difference between carbon and cellulose fibers. When the carbon fibers break, the testing machine must adjust the (displacement controlled) drive within a very short time in order to keep the strain rate of the specimen constant. Presumably, the machine's control system is not fast enough, so that the cellulose fibers experience a very high load and the specimen fails. Macroscopically, this results in a brittle fracture behavior of the cellulose-carbon samples.

The stiffness of the hybrid composites can be modeled as a good approximation as springs with different stiffnesses connected in parallel. The composite stiffness of the hybrid specimens follows very closely the mixing ratio (see Table 2) between carbon and functional fibers. The respective fiber type contributes proportionally to its amount and its fiber Young's modulus to the total stiffness of the composite. The calculation according to the rule of mixture showed a total fiber volume content of 42%. The fiber volume content calculated in this way is lower than the fiber volume content calculated using the aerial weight of the textile layers (see Table 3), since in the latter case imperfections and voids are not considered.

The changes in the material damping of the hybrid composites can be attributed to the use of the additional fiber types, since both the matrix and the manufacturing and testing conditions were kept constant. As the damping was measured at small deformations, damage and viscoplastic material behavior can be excluded as the cause of the damping. The damping is based on the viscoelastic properties of the functional fibers [4]. From the results it can be concluded that Vectran and aramid fibers have a more pronounced viscoelastic material behavior than cellulose and carbon fibers. As a result, the damping is increased through the integration of aramid and Vectran fibers.

4. Conclusions

Intraply hybridization of carbon fibers with Vectran fibers increases the material damping by up to 60% compared to samples made of pure carbon fibers. Hybridization with aramid fibers results in a small increase in damping, hybridization with cellulose fibers results in a decrease in damping compared to specimens from pure carbon fibers.

However, hybridization also leads to reduced stiffness and strength compared to a reference from pure carbon fiber: Aramid-Carbon shows the highest flexural strength of all hybrids, Aramid-Vectran the highest tensile strength. The tensile modulus of the hybrid composites is also lower than that of the non-hybrid carbon fiber reference. On the other hand, a density-specific consideration of the strength and stiffness reduces the difference between the hybrid composites and the non-hybrid carbon fiber reference. Vectran-Carbon in particular shows promising results. If the hybrid laminates are only used at selected locations in a laminate, e.g., areas with high shear [37], bicycle components can be realized with a minimal increase in weight but significantly increased material damping.

Author Contributions: Conceptualization, H.K. and C.G.; Investigation, H.K. and S.M.; Supervision, C.G. and T.G.; Writing—original draft, H.K. All authors have read and agreed to the published version of the manuscript.

Funding: This research received no external funding.

Conflicts of Interest: The authors declare no conflict of interest.

References

1. Chiementin, X.; Rigaut, M.; Crequy, S.; Bolaers, F.; Bertucci, W. Hand–arm vibration in cycling. *J. Vib. Control* **2013**, *19*, 2551–2560. [CrossRef]
2. Rivin, E.I. *Handbook on Stiffness & Damping in Mechanical Design*; American Society of Mechanical Engineers: New York, NY, USA, 2010.
3. Treviso, A.; van Genechten, B.; Mundo, D.; Tournour, M. Damping in composite materials: Properties and models. *Compos. Part B Enginering* **2015**, *78*, 144–152. [CrossRef]
4. Chandra, R.; Singh, S.; Gupta, K. Damping studies in fiber-reinforced composites—A review. *Compos. Struct.* **1999**, *46*, 41–51. [CrossRef]
5. Adams, R.D.; Bacon, D. Effect of Fibre Orientation and Laminate Geometry on the Dynamic Properties of CFRP. *J. Compos. Mater.* **1973**, *7*, 402–428. [CrossRef]
6. Adams, R.D.; Maheri, M.R. Dynamic flexural properties of anisotropic fibrous composite beams. *Compos. Sci. Technol.* **1994**, *50*, 497–514. [CrossRef]
7. Hanselka, H.; Hoffmann, U. Damping Characteristics of Fibre Reinforced Polymers. *Tech. Mech.* **1998**, *10*, 91–101.
8. Wright, G.C. The dynamic properties of glass and carbon fibre reinforced plastic beams. *J. Sound Vib.* **1972**, *21*, 205–212. [CrossRef]
9. Kretsis, G. A review of the tensile, compressive, flexural and shear properties of hybrid fibre-reinforced plastics. *Composites* **1987**, *18*, 13–23. [CrossRef]
10. Swolfs, Y.; Gorbatikh, L.; Verpoest, I. Fibre hybridisation in polymer composites: A review. *Compos. Part A Appl. Sci. Manuf.* **2014**, *67*, 181–200. [CrossRef]
11. Swolfs, Y.; McMeeking, R.M.; Verpoest, I.; Gorbatikh, L. The effect of fibre dispersion on initial failure strain and cluster development in unidirectional carbon/glass hybrid composites. *Compos. Part A Appl. Sci. Manuf.* **2015**, *69*, 279–287. [CrossRef]
12. Czél, G.; Wisnom, M.R. Demonstration of pseudo-ductility in high performance glass/epoxy composites by hybridisation with thin-ply carbon prepreg. *Compos. Part A Appl. Sci. Manuf.* **2013**, *52*, 23–30. [CrossRef]
13. Suwarta, P.; Fotouhi, M.; Czél, G.; Longana, M.; Wisnom, M.R. Fatigue behaviour of pseudo-ductile unidirectional thin-ply carbon/epoxy-glass/epoxy hybrid composites. *Compos. Struct.* **2019**, *224*, 110996. [CrossRef]
14. Pegoretti, A.; Fabbri, E.; Migliaresi, C.; Pilati, F. Intraply and interply hybrid composites based on E-glass and poly(vinyl alcohol) woven fabrics: Tensile and impact properties. *Polym. Int.* **2004**, *53*, 1290–1297. [CrossRef]
15. Fuller, J.D.; Wisnom, M.R. Pseudo-ductility and damage suppression in thin ply CFRP angle-ply laminates. *Compos. Part A Appl. Sci. Manuf.* **2015**, *69*, 64–71. [CrossRef]
16. Manders, P.W.; Bader, M.G. The strength of hybrid glass/carbon fibre composites. *J. Mater. Sci.* **1981**, *16*, 2233–2245. [CrossRef]
17. Fukunaga, H.; Chou, T.-W.; Fukuda, H. Strength of Intermingled Hybrid Composites. *J. Reinf. Plast. Compos.* **1984**, *3*, 145–160. [CrossRef]
18. Dickson, R.; Fernando, G.; Adam, T.; Reiter, H.; Harris, B. Fatigue behaviour of hybrid composites: Part 2 Carbon-g/ass hybrids. *J. Mater. Sci.* **1989**, *24*, 227–233. [CrossRef]
19. Fernando, G.; Dickson, R.; Adam, T.; Reiter, H.; Harris, B. Fatigue behaviour of hybrid composites: Part 1 Carbon/Kevlar hybrids. *J. Mater. Sci.* **1988**, *23*, 3732–3743. [CrossRef]
20. Peijs, A.; de Kok, J. Hybrid composites based on polyethylene and carbon fibres. Part 6: Tensile and fatigue behaviour. *Composites* **1993**, *24*, 19–32. [CrossRef]
21. Giancaspro, J.; Papakonstantino, C.G.; Balaguru, P.N. Flexural Response of Inorganic Hybrid Composites with E-Glass and Carbon Fibers. *J. Eng. Mater. Technol.* **2010**, *132*, 021005. [CrossRef]
22. Hosur, M.V.; Adbullah, M.; Jeelani, S. Studies on the low-velocity impact response of woven hybrid composites. *Compos. Struct.* **2005**, *67*, 253–262. [CrossRef]

23. Muñoz, R.; Martínez-Hergueta, F.; Gálvez, F.; González, C.; Llorca, J. Ballistic performance of hybrid 3D woven composites: Experiments and simulations. *Compos. Struct.* **2015**, *127*, 141–151. [CrossRef]
24. Dorey, G.; Sidey, G.R.; Hutchings, J. Impact properties of carbon fibre/Kevlar 49 fibre hydrid composites. *Composites* **1978**, *9*, 25–32. [CrossRef]
25. Swolfs, Y.; Verpoest, I.; Gorbatikh, L. Recent advances in fibre-hybrid composites: Materials selection, opportunities and applications. *Int. Mater. Rev.* **2019**, *64*, 181–215. [CrossRef]
26. Ashworth, S.; Rongong, J.; Wilson, P.; Meredith, J. Mechanical and damping properties of resin transfer moulded jute-carbon hybrid composites. *Compos. Part B Eng.* **2016**, *105*, 60–66. [CrossRef]
27. Berthelot, J.-M.; Assarar, M.; Sefrani, Y.; Mahi, A.E. Damping analysis of composite materials and structures. *Compos. Struct.* **2008**, *85*, 189–204. [CrossRef]
28. Le Guen, M.J.; Newman, R.H.; Fernyhough, A.; Emms, G.W.; Staiger, M.P. The damping–modulus relationship in flax–carbon fibre hybrid composites. *Compos. Part B Eng.* **2016**, *89*, 27–33. [CrossRef]
29. Cheour, K.; Assarar, M.; Scida, D.; Ayad, R.; Gong, X.-L. Effect of Stacking Sequences on the Mechanical and Damping Properties of Flax Glass Fiber Hybrid. *J. Renew. Mater.* **2019**, *7*, 877–889. [CrossRef]
30. Cihan, M.; Sobey, A.J.; Blake, J. Mechanical and dynamic performance of woven flax/E-glass hybrid composites. *Compos. Sci. Technol.* **2019**, *172*, 36–42. [CrossRef]
31. Davoodi, M.M.; Sapuan, S.M.; Ahmad, D.; Ali, A.; Khalina, A.; Jonoobi, M. Mechanical properties of hybrid kenaf/glass reinforced epoxy composite for passenger car bumper beam. *Mater. Des.* **2010**, *31*, 4927–4932. [CrossRef]
32. Pickering, K.L.; Efendy, M.A.; Le, T.M. A review of recent developments in natural fibre composites and their mechanical performance. *Compos. Part A Appl. Sci. Manuf.* **2016**, *83*, 98–112. [CrossRef]
33. Berthelot, J.-M.; Sefrani, Y. Damping analysis of unidirectional glass and Kevlar fibre composites. *Compos. Sci. Technol.* **2004**, *64*, 1261–1278. [CrossRef]
34. Adusumalli, R.B.; Venkateshan, K.C.; Gindl-Altmutter, W. Micromechanics of Cellulose Fibres and Their Composites. In *Wood Is Good*; Pandey, K.K., Ramakantha, V., Chauhan, S.S., Arun Kumar, A., Eds.; Springer: Singapore, 2017; pp. 299–321.
35. Buravalla, V.R.; Remillat, C.; Rongong, J.A.; Tomlinson, G.R. Advances in damping materials and technology. *Smart Mater. Bull.* **2001**, *2001*, 10–13. [CrossRef]
36. Romano, M. Charakterisierung von Gewebeverstärkten Einzellagen aus Kohlenstofffaserverstärktem Kunststoff (CFK) mit Hilfe Einer Mesomechanischen Kinematik Sowie Strukturdynamischen Versuchen. PhD Thesis, Universität der Bundeswehr München, Neubiberg, Germany, 2016.
37. Adams, R.D.; Maheri, M.R. Damping in advanced polymer–matrix composites. *J. Alloys Compd.* **2003**, *355*, 126–130. [CrossRef]